Opt Quant Electron (2018)50:5
https://doi.org/10.1007/s11082-017-1265-3

Quantum dot semiconductor optical amplifier: investigation of amplified spontaneous emission and noise figure in the presence of second excited state

Seyed Mohsen Izadyar[1] · Mohammad Razaghi[2] · Abdollah Hassanzadeh[1]

Received: 1 September 2017 / Accepted: 23 November 2017

Abstract In this paper, amplified spontaneous emission (ASE) in quantum dot semiconductor optical amplifier (QDSOA) is investigated and analyzed theoretically. The presented model is based on a set of rate equations that consider all possible carriers transitions including the second excited state (ES2). This assumption is possible, if the QDSOA's active region is grown in such a way that the presence of ES2 becomes distinguishable from upper states and wetting layer. Optical gain of QDSOA is calculated using density matrix approach. The coupled rate equations are solved numerically along with propagation equations. It is shown that in the presence of ES2, QDSOA performance can be improved and an ultra-high bit-rate signal amplification without wave distortion is possible. Furthermore, it is illustrated that the obtained ASE spectrum has three peeks which are related to ground, first excited and second excited states. Moreover, noise figure (NF) is calculated numerically using ASE power. It is shown that considering the effect of ES2 in the band diagram of quantum dots (QDs) decreases the NF of amplifier. The effect of increased input power on the reduction of NF is illustrated, too. It is shown that ASE and NF of amplifier can be ignored in the modeling QDSOA at high input powers.

Guest edited by Matthias Auf der Maur, Weida Hu, Slawomir Sujecki, Yuh-Renn Wu, Niels Gregersen, Paolo Bardella.

✉ Mohammad Razaghi
m.razaghi@uok.ac.ir

[1] Physics Department, School of Science, University of Kurdistan, Sanadaj 66177-15177, Iran

[2] Electrical Department, School of Engineering, University of Kurdistan, Sanadaj 66177-15177, Iran

Published online: 01 December 2017

Keywords Quantum dot · Semiconductor optical amplifier · Amplified spontaneous emission · Noise figure · Rate equation · Second excited state · Modeling

1 Introduction

Quantum dots (QDs) based semiconductor devices such as QD laser and QD semiconductor optical amplifier (QDSOA) have characteristics like low injection current, weak temperature sensibility and wide bandwidth gain (Akiyama et al. 2005; Sugawara and Usami 2009; Arakawa and Sakaki 1982; Bimberg 2005; Bakonyi et al. 2003). These characteristics are due to three dimensional confinement of carriers in the QDs which results in quantum size effect. Therefore, discrete energy states are appeared in the QDs. Using these semiconductor nanostructures in SOAs results in unique features like fast gain recovery, high saturation power, high optical nonlinearity, low noise figure (NF), free pattern performance, ultrahigh-speed and widely tunable wavelength conversion (Bakonyi et al. 2003; Sugawara et al. 2002; Dommers et al. 2007; Matsuura et al. 2011). Therefore, QDSOA can be a good replacement for bulk and quantum well SOAs, which are not able to process high bit-rate signals because of low gain recovery time (Sugawara et al. 2004). These features make QDSOA an ideal candidate for next generation of all optical networks.

Recombination processes in direct bandgap semiconductor devices are generally divided into two categories: radiative and non- radiative recombination. There are two types of radiative recombination which are stimulated emission (SE) and amplified spontaneous emission (ASE). ASE is one of the effective factor in low power amplification regime in SOAs. This type of emission occurs due to spontaneous recombination of electrons in conduction band (CB) and holes in valence band (VB). ASE and gain saturation are two important mechanisms that degrade the signal quality in the SOAs (Akiyama et al. 2005). Furthermore, small signal gain of SOA can be directly related to the ASE (Miao et al. 2005). Moreover, NF of SOA can be calculated numerically by analyzing ASE spectrum (Sugawara et al. 2004; Xiao and Huang 2008).

Using coupled rate equations for the carriers along with propagation equation of the input signal is one of the conventional methods to model and analyze QDSOA performance. One approach considers electrons in the CB and holes in the VB as excitons and the rate equations are written for the carriers (Bilenca and Eisenstein 2004; Sugawara et al. 2002; Daraei et al. 2013; Kolarczik et al. 2015; Nielsen and Chuang 2010). Another approach includes separate rate equations for the electrons and holes (Poel et al. 2005; Wegert et al. 2011; Zajnulina et al. 2017). In this paper, in order to involve homogeneous and inhomogeneous broadening of optical gain in the QDSOA model, an electron and a hole act as an exciton and the rate equations are written for the carriers of the CB. Furthermore, density matrix approach is used to achieve the optical gain (Sugawara et al. 2000, 2002; Sugawara 1999).

Based on the experimentally room temperature lasing report of second excited state (ES2) as well as ground state (GS) and first excited state (ES1) at high injection currents (Chen et al. 2012, 2013; Zhang et al. 2010) and structural similarity of QD laser with QDSOA, it can be assumed that ES2 be involved in the energy band diagram and rate equations of QDSOA (Izadyar et al. 2017; Razaghi et al. 2017). It can be expected that if the structure of QDSOA's active region be similar to the device structure of (Chen et al. 2012, 2013), the ES2 presence in the optical gain and ASE spectrum can be distinguished

from the upper states and WL. In this paper, for the first time, to the best of our knowledge, role of ES2 inclusion in the ASE spectrum and NF of QDSOA is studied theoretically. First result is depicted the improvement of QDSOA performance in the presence of ES2. It is shown that ultra-fast gain recovery time can be achieved, if QDs grown in such a way that the presence of ES2 could be observable in transition processes. Furthermore, propagation equation of ASE has been involved in the modeling QDSOA. ASE spectrum and NF of QDSOA are investigated by taking into consideration of ES2 in the rate equations. It is shown that in the presence of ES2, ASE spectrum has three peaks which are related to GS, ES1 and ES2. It is assumed that ES2 as well as ES1 and continuum state (CS) acts as carriers reservoir. Homogeneous and inhomogeneous broadening of optical gain spectrum are considered in the presented model, too.

This paper is organized as follow: Sect. 2 includes the theory of QDSOA based on a set of rate equations, propagation equation and calculated optical gain using density matrix approach. Furthermore, modeling method is described in this section. In Sect. 3, simulation results is illustrated and analyzed. Finally, in Sect. 4, a brief conclusion is presented.

2 Theory and modeling method

The active region of QDSOA is formed by several layers of self-assembled InAs QDs grown on GaAs substrates. Each layer is sandwiched between $Al_xGa_{1-x}As$ cladding layer. The operational wavelength of this QDSOA is 1.3 μm (Nakata et al. 2000; Liu et al. 2004; Mukai et al. 2000; Schmidt et al. 1996). In this paper, it is assumed that ten layers of self-assembled QDs are in the active region of the amplifier (Sugawara et al. 2004). The self-assemled QDs can be grown via the Stranski–Krastanow growth mode under highly mismatched molecular beam epitaxy (MBE) (Kovsh et al. 2003) on a substrate called wetting layer (WL). They form dot-in-well (DWELL) structures (Kovsh et al. 2003; Stintz et al. 2000). The grown procedure of the QDs results in size distribution of dots and therefore, an inhomogeneous broadening of optical gain spectrum (Bilenca and Eisenstein 2004; Sugawara et al. 2005; Chow et al. 2015; Asryan and Suris 1996).

In order to model QDSOA, a set of rate equations is written for the carriers in the GS, upper states and WL (Sugawara et al. 2002, 2004, 2005; Xiao and Huang 2008). Furthermore, propagation equations of the input signal and ASE are coupled with the rate equations. Therefore, these equations should be solved to investigate ASE spectrum in the QDSOA. In the modeling ASE spectrum and NF of QDSOA, for the first time, to the best of our knowledge, the effect of ES2 inclusion is investigate in the rate equations (Izadyar et al. 2017; Razaghi et al. 2017). The band diagram of QDs in different group dots and related transitions of the carriers are depicted in Fig. 1. It is assumed that QDs are spatially isolated. In other words, each dot can exchange carriers only with WL. The homogeneous and inhomogeneous broadening of the optical gain have been considered in the model by grouping dots based on interband transition resonant frequency of GS between the carriers of CB and VB. The homogeneous broadening is due to the intrinsic gain of a single dot. The inhomogeneous broadening is due to the size distribution of QDs arisen from growth method. QDs and photon modes are divided into $4M + 2$ groups to include the entire frequency range of ASE spectrum. The QDSOA is modeled based on the following equations. In the following equations, the indexes of w, c, $e2$, $e1$ and g are related to WL, CS, ES2, ES1 and GS, respectively.

The resonant frequency of jth group dots is given as:

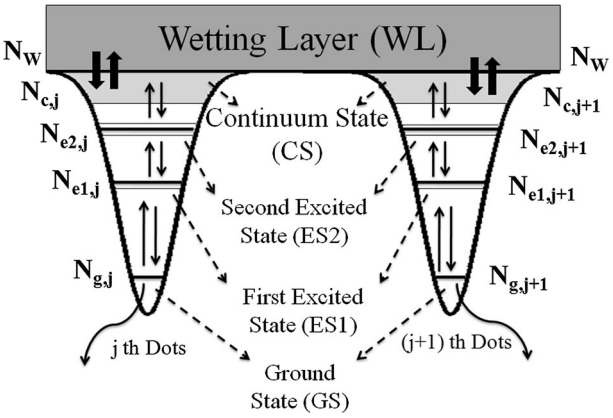

Fig. 1 Band diagram of self-assembled QD's conduction band (CB) in different group dots based on the interband transition resonant frequency of GS between CB and VB

$$\omega_j^s = \omega_{cv}^s - (M - j)\Delta\omega \tag{1}$$

where ω_{cv}^s is the central resonant frequency of the inhomogeneous broadening for the GS, ES1 and ES2. The index of s is related to g, $e1$ and $e2$. M is an integer number and is chosen to be 400 (Izadyar et al. 2017). $\Delta\omega$ is the frequency space between the groups and $j = 1, 2, \ldots, 4M + 2$. The optical gain of the QDs in the jth group, which is calculated using density matrix approach (Sugawara 1999), is given by:

$$g_{m,j}^s(t, \omega_m^s, N_j^s) = \frac{2\pi e^2 N_D |P_{cv}^\sigma|^2}{\varepsilon_0 c n_{eff} m_0^2 \hbar \omega_{cv}^s} G_j D_s B(\omega_m - \omega_j^s)(2P_j^s - 1) \tag{2}$$

where $g_{m,j}^s(t, \omega_m^s, N_j^s)$ is the optical gain of the QDs in the jth group at frequency of ω_m^s for the GS, ES1 and ES2, e is the elementary charge of electron, $|P_{cv}^\sigma|$ is the transition matrix element for σ polarization (Sugawara et al. 2000), ε_0 is the permittivity of vacuum, c is the speed of light in vacuum, n_{eff} is the effective refractive index of the active region, m_0 is the free electron mass and $\hbar$ is the reduced Planck constant. G_j is a normalized inhomogeneous broadening function with Gaussian distribution (Sugawara et al. 2000; Izadyar et al. 2017). $B(\omega_m - \omega_j^s)$ is the homogeneous broadening function with a Lorentz shape (Sakamoto and Sugawara 2000). Two dimensional coverage of dots which is related to the QDs density, N_D, and their volume, V_D, by $\xi = N_D V_D$ is considered to be 0.1 and 0.15 (Sugawara et al. 2000, 2002). The optical gain of ASE, $g_{sp,j}^s(t, \omega_{sp}^s, N_j^s)$, is considered to be equal with $g_{m,j}^s(t, \omega_{sp}^s, N_j^s)$ expect $(2P_j^s - 1)$ replaced by $(P_j^s)^2$. The occupation probability of the jth dots in the s state, P_j^s, is determined by the balance between the rates of carrier relaxation, carrier excitation and photon emission. According to Pauli's exclusion principle, the probability of P is related to the carrier density of N as:

$$P_j^s = \frac{N_j^s}{2D_s N_D G_j} \tag{3}$$

where D_s is defined as the degeneracy of GS, ES1, ES2 and CS.

The propagation equation of the input signal as a function of reduced time, τ, and propagation direction, z, for the mth photon mode is given as:

$$\frac{dS_m^s(z,\tau)}{dz} = \left[\Gamma \sum_{j=1}^{2M+1} g_{m,j}^s(\tau, \omega_m^s, N_j^s) - \alpha_{loss}\right] S_m^s(z,\tau) \tag{4}$$

where α_{loss} is the internal loss of the cavity and $\tau = t - \frac{n_r z}{c}$. The propagation equation has been written for a single-pass travelling-wave SOA (Agrawal and Olsson 1989; Sugawara et al. 2004; Radziunas et al. 2015).

The optical gain and ASE spectrum in the QDs are strongly polarization dependent. For simplicity, the spontaneous emission of transverse-magnetic (TM) polarization is ignored. Because, ASE with TM polarization is much smaller than that of transverse-electric (TE) polarization (Xiao and Huang 2008). The propagation equation of ASE with TE polarization at ω_{sp} frequency obeys the following equation:

$$\frac{dS_{sp}}{dz} = \left[\Gamma \sum_{j=1}^{2M+1} g_{m,j}(z,\tau,\omega_m) - \alpha_{loss}\right] S_{sp} + \Gamma \sum_{j=1}^{2M+1} g_{sp}(z,\tau,\omega_m) S_{vac}(\omega_{sp}) \tag{5}$$

where photon flux density of the vacuum field, $S_{vac}(\omega_{sp})$, with a frequency between ω_{sp} and $\omega_{sp} + \Delta\omega_{sp}$ is given as:

$$S_{vac} = \frac{\Delta\omega_{sp}}{2\pi D} \tag{6}$$

D is the cross section area of the QDSOA's active region and $\Delta\omega_{sp} = 2\pi\Delta f_{sp}$ is the frequency mode spacing of the ASE spectrum.

The rate equations of the carriers in the WL and CS are given, respectively, as:

$$\frac{dN_w(z,t)}{dt} = \frac{J}{ed} - \frac{N_w(z,t)}{\overline{\tau}_{wc}} - \frac{N_w(z,t)}{\tau_{wr}} + \frac{\sum_j N_{c,j}(z,t)}{\tau_{cw}} \tag{7}$$

$$\begin{aligned}\frac{dN_{c,j}(z,t)}{dt} = {} & \frac{G_j N_w(z,t)}{\tau_{wc,j}} + \frac{N_{g,j}(z,t)}{\tau_{gc,j}} + \frac{N_{e1,j}(z,t)}{\tau_{e1c,j}} + \frac{N_{e2,j}(z,t)}{\tau_{e2c,j}} - \frac{N_{c,j}(z,t)}{\tau_{cg,j}} \\ & - \frac{N_{c,j}(z,t)}{\tau_{ce1,j}} - \frac{N_{c,j}(z,t)}{\tau_{ce2,j}} - \frac{N_{c,j}(z,t)}{\tau_{cw}} - \frac{N_{c,j}(z,t)}{\tau_r}\end{aligned} \tag{8}$$

The rate equations of the carries in the ES2, ES1 and GS are given, respectively, as:

$$\begin{aligned}\frac{dN_{e2,j}(z,t)}{dt} = {} & \frac{N_{c,j}(z,t)}{\tau_{ce2,j}} + \frac{N_{e1,j}(z,t)}{\tau_{e1e2,j}} + \frac{N_{g,j}(z,t)}{\tau_{ge2,j}} - \frac{N_{e2,j}(z,t)}{\tau_{e2c,j}} - \frac{N_{e2,j}(z,t)}{\tau_{e2e1,j}} \\ & - \frac{N_{e2,j}(z,t)}{\tau_{e2g,j}} - \frac{N_{e2,j}(z,t)}{\tau_r} - \frac{c}{n_r}\Gamma \sum_m g_{m,j}^{e2}(t, \omega_m^{e2}, N_j^{e2}) S_m^{e2}(z,t) \\ & - \frac{c}{n_r}\Gamma \sum_m g_{sp,j}^{e2}(t, \omega_m^{e2}, N_j^{e2}) S_{sp}^{e2}(z,t)\end{aligned} \tag{9}$$

$$\frac{dN_{e1,j}(z,t)}{dt} = \frac{N_{c,j}(z,t)}{\tau_{ce1,j}} + \frac{N_{e2,j}(z,t)}{\tau_{e2e1,j}} + \frac{N_{g,j}(z,t)}{\tau_{ge1,j}} - \frac{N_{e1,j}(z,t)}{\tau_{e1c,j}} - \frac{N_{e1,j}(z,t)}{\tau_{e1e2,j}} - \frac{N_{e1,j}(z,t)}{\tau_{e1g,j}} - \frac{N_{e1,j}(z,t)}{\tau_r} - \frac{c}{n_r}\Gamma\sum_m g^{e1}_{m,j}(t,\omega^{e1}_m,N^{e1}_j)S^{e1}_m(z,t) - \frac{c}{n_r}\Gamma\sum_m g^{e1}_{sp,j}(t,\omega^{e1}_m,N^{e1}_j)S^{e1}_{sp}(z,t) \tag{10}$$

$$\frac{dN_{g,j}(z,t)}{dt} = \frac{N_{g,j0}(z,t) - N_{g,j}(z,t)}{\tau_{eff,j}(z,t)} - \frac{c}{n_r}\Gamma\sum_m g^{g}_{m,j}(t,\omega^{g}_m,N^{g}_j)S^{g}_m(z,t) - \frac{c}{n_r}\Gamma\sum_m g^{g}_{sp,j}(t,\omega^{g}_m,N^{g}_j)S^{g}_{sp}(z,t) \tag{11}$$

where J is the current density, d is the WL thickness, τ_{cw} is the carrier escape time from CS to WL and Γ is the optical confinement factor. $\tau_{ge1,j}$, $\tau_{ge2,j}$, $\tau_{gc,j}$, $\tau_{e1e2,j}$, $\tau_{e1c,j}$ and $\tau_{e2c,j}$ are the carrier excitation lifetimes of the jth group dots from the lower states to the upper states (Izadyar et al. 2017). First index refers to the lower state and second index refers to the upper state. τ_{wr} and τ_r are recombination lifetime of the carriers in the WL and QDs, respectively, which are due to the radiative, non- radiative and Auger recombination processes (Sugawara et al. 2002). $\tau_{wc,j}$, $\tau_{cg,j}$, $\tau_{ce1,j}$, $\tau_{ce2,j}$, $\tau_{e2g,j}$, $\tau_{e2e1,j}$ and $\tau_{e1g,j}$ are the carrier relaxation time from the upper states to the jth group dots of the lower states. First index refers to the upper state and second index refers to the lower state. Because the carrier relaxation is prevented by the state filling according to the exclusion principle, the relaxation rate is defined as $\tau^{-1} = (1 - P^s)\tau_0^{-1}$, where τ_0 is the relaxation rate when the s state is unoccupied (Izadyar et al. 2017). The relaxation lifetimes of the different states are assumed to be equal and defined as $\tau_{cg,0} = \tau_{ce1,0} = \tau_{ce2,0} = \tau_{e2g,0} = \tau_{e2e1,0} = \tau_{e1g,0} = \tau_d$. The carrier relaxation lifetime in the self-assembled QDs is usually obtained based on the Auger effect (Adler et al. 1996; Uskov et al. 1997). In this study, the effect of Auger-related relaxation processes is summarized in relaxation lifetime, τ_d, which can be between 0.5 and 100 ps (Sugawara et al. 2002). The carrier density of the GS in the steady state condition is defined as:

$$N_{g,j0} = \left(\frac{N_{c,j}(z,t)}{\tau_{cg,0}} + \frac{N_{e2,j}(z,t)}{\tau_{e2g,0}} + \frac{N_{e1,j}(z,t)}{\tau_{e1g,0}}\right)\tau_{eff,j}(z,t) \tag{12}$$

where $\tau_{eff,j}$ is the response time of the gain saturation and is given as:

$$\tau_{eff,j}(z,t) = \left(\frac{N_{c,j}(z,t)}{2N_D G_j \tau_{cg,0}} + \frac{N_{e2,j}(z,t)}{2N_D G_j \tau_{e2g,0}} + \frac{N_{e1,j}(z,t)}{2N_D G_j \tau_{e1g,0}} + \frac{1}{\tau_{gc,j}} + \frac{1}{\tau_{ge2,j}} + \frac{1}{\tau_{ge1,j}} + \frac{1}{\tau_r}\right)^{-1} \tag{13}$$

The NF of QDSOA based on the ASE spectrum is defined as:

$$NF = \frac{1 + 2\eta_{out}S_{sp}(L,\tau,\omega_m)/S_{vac}(\omega_m)}{\eta_{in}\eta_{out}G^{(1)}(\tau)} \tag{14}$$

where η_{in} and η_{out} are the input and output coupling coefficient, respectively and $G^{(1)}(\tau)$ is the linear amplifier gain.

In order to model and analyze the QDSOA, the set of carrier's rate equations (Eqs. 7–11) along with the propagation equations of the input signal and ASE (Eqs. 4 and 5) in the cavity should be solved simultaneously. An analytical solution of these equations is extremely complicated and hardly possible. Therefore, rate equations and propagation equations should be solved numerically. Carriers in each state have $2M + 1$ rate equations and $4M + 2$ resonant frequency mode (Eq. 1 and related equations). Therefore, $8M + 5$ rate equations with $4M + 2$ propagation equations should be calculated numerically to analyze QDSOA performance. It is assumed that signal amplification is due to the carrier recombination in GS of CB and VB. Upper states act as carrier reservoir. For simplicity, the length of QDSOA is divided into smaller sections to vanish the spatial dependency of the optical gain and carrier density in Eqs. 4 and 5. In this case, the propagation equation of the input signal takes an exponential form in each section to amplify the signal through the cavity length. Therefore, numerical solution of the rate equations with the fourth-order Runge–Kutta method is used in each section for all cavity modes simultaneously to evaluated the ASE spectrum in the QDSOA. In other word, exponential amplification of output signal in one section is considered as input signal for the next section and therefore, rate equations are solved numerically in this section. The number of these time-dependent rate equations with $M = 400$ is 3205. However, the numerical solution method for these number of rate equations is complex and extremely time consuming. Some parameters used in the calculations are listed in Table 1.

Table 1 Parameters which are used in the calculation and simulation

Parameter	Symbol	Value
Internal loss of cavity	α_{loss}	5 cm^{-1}
Active region length	L	1200 μm
Active region width	w	1.5 μm
Band gap	E_g	0.8 eV
Central transition energy of GS	E_{cv}^{g}	0.9493 eV
Central transition energy of ES1	E_{cv}^{e1}	1.0221 eV
Central transition energy of ES1	E_{cv}^{e2}	1.0763 eV
Input coupling coefficient	η_{in}	−2 dB
Output coupling coefficient	η_{out}	−2 dB
Number of QDs layers	N_l	10
Optical confinement factor	Γ	0.10
Carrier recombination lifetimes in dots	τ_r	1 ns
Carrier recombination lifetimes in WL	τ_{wr}	0.4 ns
frequency mode spacing	Δf_{sp}	100 GHz
FWHM of homogeneous broadening function	Γ_{cv}	10 meV
Degeneracy of GS (Sugawara et al. 2004)	D_g	1
Degeneracy of ES1 (Sugawara et al. 2004)	D_{e1}	3
Degeneracy of ES2 (Sugawara et al. 2004)	D_{e2}	6
Degeneracy of CS (Sugawara et al. 2004)	D_c	10
Temperature	T	295 K

3 Simulation results

First result has been obtained to show the improvement of QDSOA performance in the presence of ES2. Figure 2 shows the optical gain, amplified signal and normalized output signal as a function of time for a Gaussian pulse train in three cases: without ES2 at relaxation lifetime of $\tau_d = 10$ ps and with ES2 at two different relaxation lifetimes of $\tau_d = 5$ and 10 ps. Input pulse width is 500 fs and peak power is 40 mW, which give the average power of 21.3 mW. At this input power, QDSOA works in the nonlinear regime under spectral hole burning (SHB) (Sugawara et al. 2002; Izadyar et al. 2017). This pulse train has the bit-rate of 450 Gbps. Simulation parameters are the same as Table 1 expect $D_{e1} = 6$, $D_{e2} = 9$, $D_c = 20$, $\Gamma = 0.15$ and $\xi = 0.15$ (Sugawara et al. 2002). As it can be seen in Fig. 2a, maximum optical gain is 520 cm^{-1}, which is in good agreement with the experimental results (Hatori et al. 2000).

As it has been illustrated in Fig. 2a, gain saturation and recovery time have decreased in the presence of ES2. The ES2 inclusion in the QDSOA improves the signal amplification (see Fig. 2b) and reduces peak shift of the amplified signal (see Fig. 2c). Furthermore, by

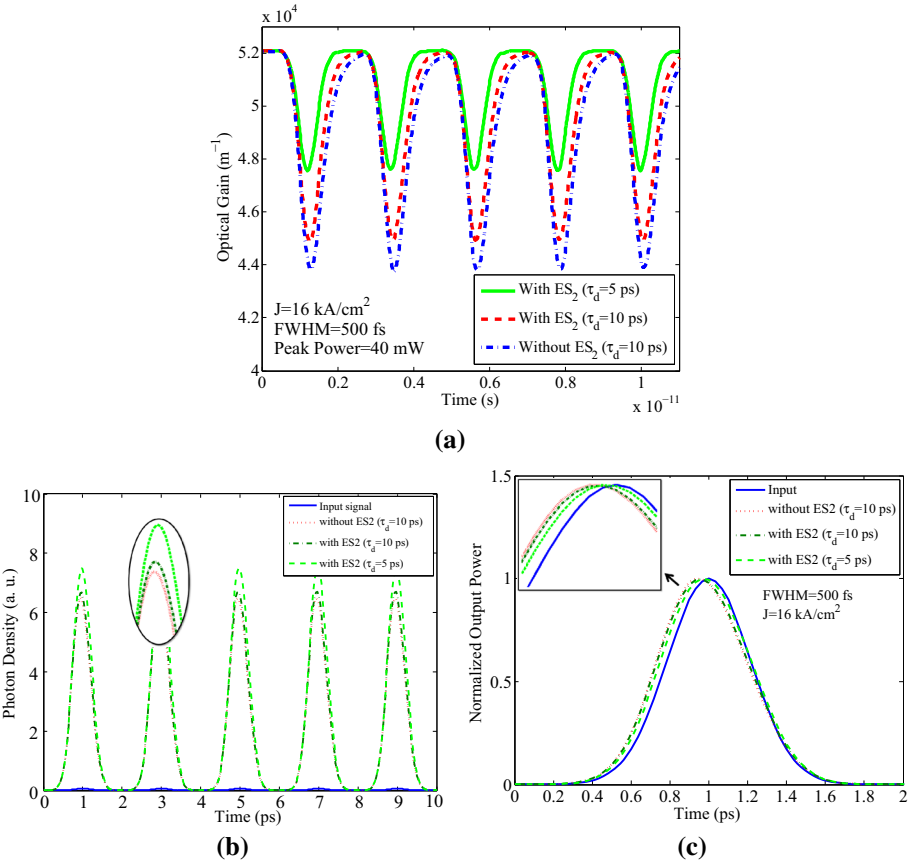

Fig. 2 Amplification of input Gaussian pulse train. **a** optical gain, **b** photon density and **c** normalized output power of one pulse, as a function of time. Bit-rate is 450 Gbps

reducing the relaxation lifetime, τ_d, the gain recovery time and the gain saturation have decreased and the signal amplification and peak shift have improved further. Therefore, ultra-high bit-rate signal amplification up to 450 Gbps without wave distortion becomes possible.

In order to show peaky behavior in the ASE spectrum, it is supposed that the SOA is biased by a high level injection current density of 24 kA/cm^2, before the input signal is entered to the cavity. Then, the injection current is decreased to 1 kA/cm^2 in the beginning of the amplification process. This case is called as high-to-low injection regime. In this regime, due to high level injection, the upper states are filled completely before the amplification process. Therefore, due to high optical and ASE gain at $J = 24$ kA/cm^2 at the central resonant frequency of ES2, the output signal and ASE of ES2 peak powers are considerably high.

Figure 3a illustrates the ASE power of QDSOA in the presence and absence of ES2 at high-to-low injection regime. The case without ES2 has been depicted just for comparison. Figure 3b shows the ASE spectrum for two cases: low-to-high and high-to-low injection regimes. In these figure, $J = 1$ kA/cm^2, $\tau_d = 10$ ps and $\xi = 0.10$. Other parameters are the

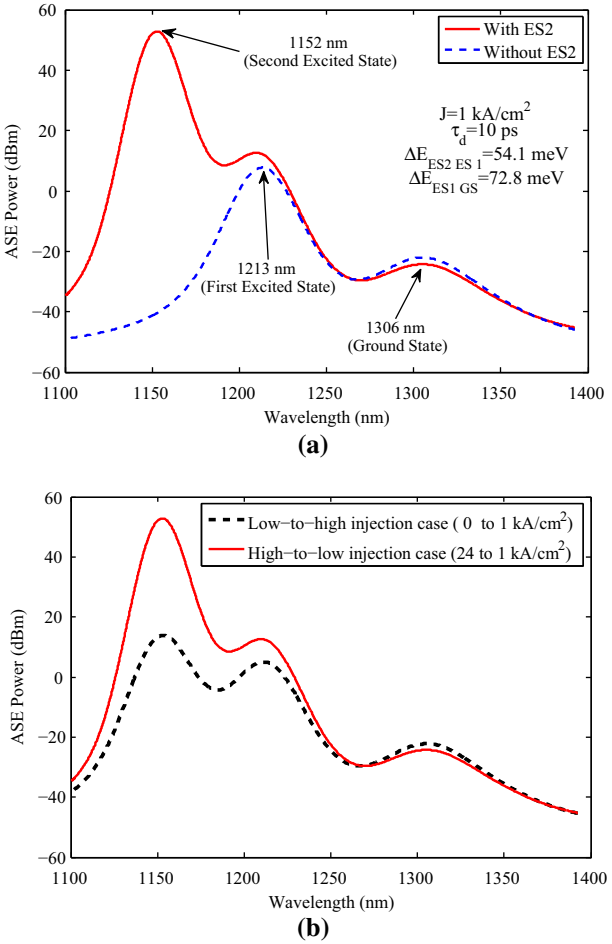

Fig. 3 ASE power as a function of wavelength, **a** in the presence and absence of ES2 at high-to-low injection regime. **b** in the presence of ES2 at two cases: high-to-low and low-to-high injection current densities

same as those listed in Table 1. As it can be seen in Fig. 3a, in the presence of ES2, there are three peaks which are related to GS, ES1 and ES2. The central resonant frequency of GS, ES1 and ES2 are related to the peaks at wavelength of 1306, 1213 and 1152 nm, respectively. As mentioned before, it is assumed that signal amplification is only due to the recombination of carriers in the GS of CB and VB. Upper states act as carrier reservoir. Therefore, input signals which are propagated at the wavelength of 1306 nm is amplified. As it can be seen, ASE power of ES2 peak is very high (about 52 dBm). The main reason of such a high ASE power at high-to-low injection regime is due to the ES2 related QD's parameters like its resonant energy and degeneracy. The effect of these parameters appear in the optical gain equation (Eq. 2). Therefore, optical gain and ASE gain are increased drastically and therefore, ASE power is increased intensely (see Eqs. 2 and 5). Although, in the low-to-high injection regime (0–1 kA/cm^2), the upper states are not filled and therefore, the optical gain and ASE gain are decreased due to the reduced occupation probability (see Eqs. 2 and 3). Therefore, output and ASE power are decreased intensely. The results shown that in this case can be verified through comparison with experimental results (Xiao and Huang 2008).

In order to compare the obtained results with previous works, the NF of QDSOA in the case without ES2 is calculated using the obtained ASE power spectrum with the parameters listed in Table 1. The NF is calculated at the wavelength of 1306 nm and at low input powers. For $J = 1$–16 kA/cm^2 the NF in the linear region is approximately constant and equal to 5.68 dB which is the same as (Sugawara et al. 2004). But in the presence of ES2, the NF decreases to 4.67 dB for the same current densities which is comparable with the experimental results reported in (Akiyama et al. 2005).

Figure 4 shows the NF of QDSOA as a function of wavelength at low-to-high injection regime. In this figure, the NF spectrum is depicted for the input continuous wave (CW) powers of − 10, − 6.66, − 3.33 and 16.67 dBm at $J = 1$ kA/cm^2. The NF of GS resonant wavelength are changed slightly at low input powers, but at high input powers (nonlinear working region of QDSOA), the change in the NF becomes distinguishable. As it can be seen, by increasing the input power, the NF of QDSOA is decreased at short wavelength side, which is in good agreement with (Xiao and Huang 2008). The NF spectrum has one peak at wavelength of 1152 nm which is related to ES2 resonant wavelength. Although, at

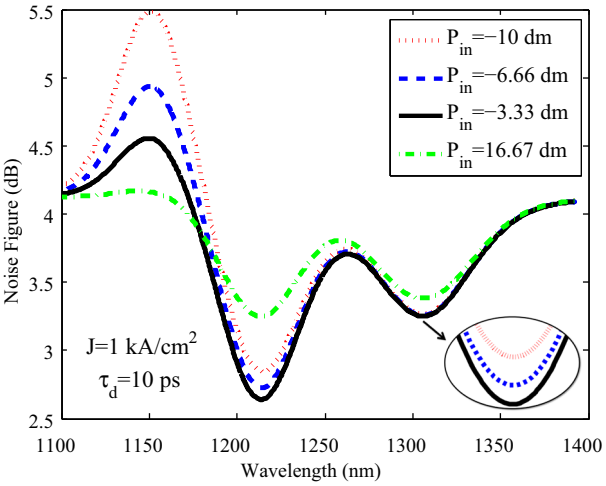

Fig. 4 Noise Figure (NF) of QDSOA as a function of wavelength. Input CW powers are $P_{in} = -10, -6.66, -3.33$ and 16.67 dBm. This figure has been depicted at low-to-high injection regime (0–1 kA/cm^2)

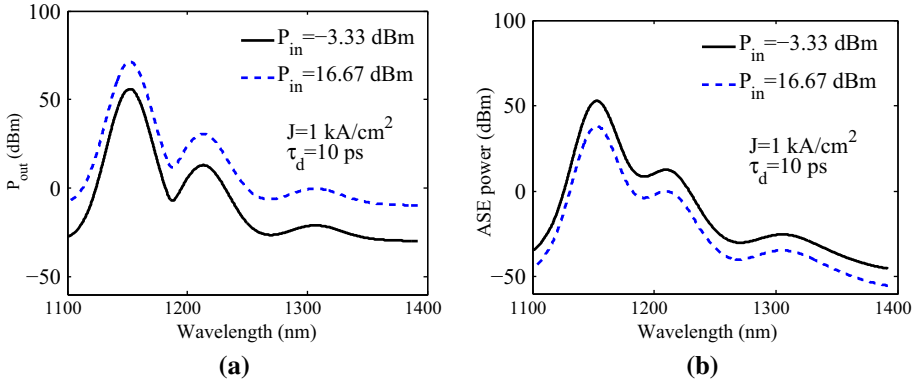

Fig. 5 Output power and ASE spectrum at $J = 1$ kA/cm^2 for input power of − 3.33 and 16.67 dBm.

resonant wavelengths of GS and ES1, there is no peak. Because upper states act as a carrier reservoir. Therefore, in this case, upper states are not filled completely and various behavior of NF in these states are due to their different inversions. On the other hand, the peak of ES2 is due to intensely increased ASE power because of degeneracy parameter, D_{e2}, (see Fig. 3a). The NF of 1306 nm wavelength at high-to-low injection regime at input power of − 3.33 dBm is about 4.67 dB and at input power of 16.67 dBm is decreased to 3.6 dB.

In order to show the effect of input power on the ASE spectrum, the output power and ASE spectrum are depicted in Fig. 5. In this figure, $J = 1$ kA/cm^2 and the input powers are − 3.33 and 16.67 dBm. This figure is obtained at high-to-low injection regime. As expected, increasing input power results in an increase of the output power (see Fig. 5a), but high input power results in a decrease of ASE power (see Fig. 5b). In other words, as it can be seen in Figs. 4 and 5, at high input powers, the effects of ASE and NF can be ignored in the modeling of QDSOA due to negligible ASE and NF of the amplifier.

4 Conclusion

In this paper, a theoretical model was presented to investigate and analyze the ASE spectrum and NF of QDSOA. This model was based on a set of rate equations and density matrix approach along with the propagation equations of the input signal and ASE. For the first time, to the best of our knowledge, ASE spectrum in QDSOA was obtained by considering the effect of ES2 inclusion in the band diagram of QDs and the optical transitions of the carriers. This assumption was due to the experimentally three-state lasing report of QD laser in the room temperature. It was assumed that if the structure of QDSOA's active region is similar to this QD laser, presence of ES2 in the gain spectrum could be distinguished from the upper states and WL. It was shown that QDSOA performance could be improved in the presence of ES2. It was illustrated that ultra-high bit-rate signal processing up to 450 Gbps was possible in the presence of ES2 without wave distortion. Furthermore, it was shown that ASE spectrum has three peaks which are related to resonant frequency of GS, ES1 and ES2. It was obtained that NF could be decreased in the presence of ES2. NF of 4.67 dB was calculated in the presence of ES2, while NF without ES2 was calculated 5.68 dB. NF spectrum was depicted to show the wavelength

dependency of NF. It was shown that the NF of QDSOA was decreased by increasing input CW power. At resonant wavelength of GS, increasing input power resulted in minimizing the NF of the amplifier. Furthermore, at high input powers, ASE power was decreased further. Therefore, it could be conclude that ASE and NF were reduced at high input powers. In other words, ASE and NF could be ignored in the modeling of QDSOA performance at high input powers which QDSOA works in nonlinear region.

References

Adler, F., Geiger, M., Bauknecht, A., Scholz, F., Schweizer, H., Pilkuhn, M., Ohnesorge, B., Forchel, A.: Optical transitions and carrier relaxation in self assembled InAs/GaAs quantum dots. J. Appl. Phys. **80**(7), 4019–4026 (1996)

Agrawal, G.P., Olsson, N.A.: Self-phase modulation and spectral broadening of optical pulses in semiconductor laser amplifiers. IEEE J. Quantum Electron. **25**(11), 2297–2306 (1989)

Akiyama, T., Ekawa, M., Sugawara, M., Kawaguchi, K., Sudo, H., Kuramata, A., Ebe, H., Arakawa, Y.: An ultrawide-band semiconductor optical amplifier having an extremely high penalty-free output power of 23 dbm achieved with quantum dots. IEEE Photonics Technol. Lett. **17**(8), 1614–1616 (2005)

Arakawa, Y., Sakaki, H.: Multidimensional quantum well laser and temperature dependence of its threshold current. Appl. Phys. Lett. **40**(11), 939–941 (1982)

Asryan, L., Suris, R.: Inhomogeneous line broadening and the threshold current density of a semiconductor quantum dot laser. Semicond. Sci. Technol. **11**(4), 554–567 (1996)

Bakonyi, Z., Su, H., Onishchukov, G., Lester, L.F., Gray, A.L., Newell, T.C., Tunnermann, A.: High-gain quantum-dot semiconductor optical amplifier for 1300 nm. IEEE J. Quantum Electron. **39**(11), 1409–1414 (2003)

Bilenca, A., Eisenstein, G.: On the noise properties of linear and nonlinear quantum-dot semiconductor optical amplifiers: the impact of inhomogeneously broadened gain and fast carrier dynamics. IEEE J. Quantum Electron. **40**(6), 690–702 (2004)

Bimberg, D.: Quantum dots for lasers, amplifiers and computing. J. Phys. D Appl. Phys. **38**(13), 2055–2058 (2005)

Chen, S., Zhou, K., Zhang, Z., Childs, D., Hugues, M., Ramsay, A., Hogg, R.: Ultra-broad spontaneous emission and modal gain spectrum from a hybrid quantum well/quantum dot laser structure. Appl. Phys. Lett. **100**(4), 041118 (2012a)

Chen, S., Zhou, K., Zhang, Z., Wada, O., Childs, D., Hugues, M., Jin, X., Hogg, R.: Room temperature simultaneous three-state lasing in hybrid quantum well/quantum dot laser. Electron. Lett. **48**(11), 644–645 (2012b)

Chen, S., Zhou, K., Zhang, Z., Orchard, J.R., Childs, D.T., Hugues, M., Wada, O., Hogg, R.A.: Hybrid quantum well/quantum dot structure for broad spectral bandwidth emitters. IEEE J. Sel. Top. Quantum Electron. **19**(4), 1900209–1900209 (2013)

Chow, W.W., Liu, A.Y., Gossard, A.C., Bowers, J.E.: Extraction of inhomogeneous broadening and non-radiative losses in inas quantum-dot lasers. Appl. Phys. Lett. **107**(17), 171106 (2015)

Daraei, A., Izadyar, S.M., Chenarani, N.: Simulation and analysis of carrier dynamics in the inas/gaas quantum dot laser, based upon rate equations. Opt. Photonics J. **3**(01), 112–116 (2013)

Dommers, S., Temnov, V.V., Woggon, U., Gomis, J., Martinez-Pastor, J., Laemmlin, M., Bimberg, D.: Complete ground state gain recovery after ultrashort double pulses in quantum dot based semiconductor optical amplifier. Appl. Phys. Lett. **90**(3), 033508 (2007)

Hatori, N., Sugawara, M., Mukai, K., Nakata, Y., Ishikawa, H.: Room-temperature gain and differential gain characteristics of self-assembled ingaas/gaas quantum dots for 1.1-1.3 μm semiconductor lasers. Appl. Phys. Lett. **77**(6), 773–775 (2000)

Izadyar, S.M., Razaghi, M., Hassanzadeh, A.: Quantum dot semiconductor optical amplifier: role of second excited state on ultrahigh bit-rate signal processing. Appl. Opt. **56**(12), 3599–3607 (2017)

Kolarczik, M., Owschimikow, N., Herzog, B., Buchholz, F., Kaptan, Y.I., Woggon, U.: Exciton dynamics probe the energy structure of a quantum dot-in-a-well system: the role of coulomb attraction and dimensionality. Phys. Rev. B **91**(23), 235310 (2015)

Kovsh, A., Maleev, N., Zhukov, A., Mikhrin, S., Vasil'ev, A., Semenova, E., Shernyakov, Y.M., Maximov, M., Livshits, D., Ustinov, V., et al.: Inas/ingaas/gaas quantum dot lasers of 1.3 μm range with enhanced optical gain. J. Cryst. Growth **251**(1), 729–736 (2003)

Liu, H., Sellers, I., Badcock, T., Mowbray, D., Skolnick, M., Groom, K., Gutierrez, M., Hopkinson, M., Ng, J., David, J., et al.: Improved performance of 1.3 μm multilayer inas quantum-dot lasers using a high-growth-temperature gaas spacer layer. Appl. Phys. Lett. **85**(5), 704–706 (2004)

Matsuura, M., Raz, O., Gomez-Agis, F., Calabretta, N., Dorren, H.J.: Ultrahigh-speed and widely tunable wavelength conversion based on cross-gain modulation in a quantum-dot semiconductor optical amplifier. Opt. Express **19**(26), B551–B559 (2011)

Miao, Q., Huang, D., Liu, D., Wang, T., Zeng, X.: Rapid evaluation of gain spectra from measured ASE spectra of travelling-wave semiconductor optical amplifier. Chin. Opt. Lett. **3**(8), 483–485 (2005)

Mukai, K., Nakata, Y., Otsubo, K., Sugawara, M., Yokoyama, N., Ishikawa, H.: 1.3 μm cw lasing characteristics of self-assembled ingaas-gaas quantum dots. IEEE J. Quantum Electron. **36**(4), 472–478 (2000)

Nakata, Y., Mukai, K., Sugawara, M., Ohtsubo, K., Ishikawa, H., Yokoyama, N.: Molecular beam epitaxial growth of inas self-assembled quantum dots with light-emission at 1.3 μm. J. Cryst. Growth **208**(1), 93–99 (2000)

Nielsen, D., Chuang, S.L.: Four-wave mixing and wavelength conversion in quantum dots. Phys. Rev. B **81**(3), 035305 (2010)

Radziunas, M., Herrero, R., Botey, M., Staliunas, K.: Far-field narrowing in spatially modulated broad-area edge-emitting semiconductor amplifiers. JOSA B **32**(5), 993–1000 (2015)

Razaghi, M., Izadyar, S.M., Madanifar, K.A.: Investigation of amplified spontaneous emission in quantum dot semiconductor optical amplifier in presence of second excited state. In: 2017 International Conference on Numerical Simulation of Optoelectronic Devices (NUSOD), IEEE, pp. 37–38 (2017)

Sakamoto, A., Sugawara, M.: Theoretical calculation of lasing spectra of quantum-dot lasers: effect of homogeneous broadening of optical gain. IEEE Photonics Technol. Lett. **12**(2), 107–109 (2000)

Schmidt, K., Medeiros-Ribeiro, G., Oestreich, M., Petroff, P., Döhler, G.: Carrier relaxation and electronic structure in inas self-assembled quantum dots. Phys. Rev. B **54**(16), 11346–11353 (1996)

Stintz, A., Liu, G., Li, H., Lester, L., Malloy, K.: Low-threshold current density 1.3-μm inas quantum-dot lasers with the dots-in-a-well (dwell) structure. IEEE Photonics Technol. Lett. **12**(6), 591–593 (2000)

Sugawara, M.: Self-assembled InGaAs/GaAs Quantum Dots, vol. 60. Academic Press, London (1999)

Sugawara, M., Usami, M.: Quantum dot devices: handling the heat. Nat. Photonics **3**(1), 30–31 (2009)

Sugawara, M., Mukai, K., Nakata, Y., Ishikawa, H., Sakamoto, A.: Effect of homogeneous broadening of optical gain on lasing spectra in self-assembled in_x ga_{1-x} as/gaas quantum dot lasers. Phys. Rev. B **61**(11), 7595–7603 (2000)

Sugawara, M., Akiyama, T., Hatori, N., Nakata, Y., Ebe, H., Ishikawa, H.: Quantum-dot semiconductor optical amplifiers for high-bit-rate signal processing up to 160 gbs^{-1} and a new scheme of 3r regenerators. Meas. Sci. Technol. **13**(11), 1683–1691 (2002)

Sugawara, M., Ebe, H., Hatori, N., Ishida, M., Arakawa, Y., Akiyama, T., Otsubo, K., Nakata, Y.: Theory of optical signal amplification and processing by quantum-dot semiconductor optical amplifiers. Phys. Rev. B **69**(23), 235332 (2004)

Sugawara, M., Hatori, N., Ebe, H., Ishida, M., Arakawa, Y., Akiyama, T., Otsubo, K., Nakata, Y.: Modeling room-temperature lasing spectra of 1.3-μm self-assembled inas/ gaas quantum-dot lasers: homogeneous broadening of optical gain under current injection. J. Appl. Phys. **97**(4), 043523 (2005)

Uskov, A., Adler, F., Schweizer, H., Pilkuhn, M.: Auger carrier relaxation in self-assembled quantum dots by collisions with two-dimensional carriers. J. Appl. Phys. **81**(12), 7895–7899 (1997)

van der Poel, M., Gehrig, E., Hess, O., Birkedal, D., Hvam, J.M.: Ultrafast gain dynamics in quantum-dot amplifiers: theoretical analysis and experimental investigations. IEEE J. Quantum Electron. **41**(9), 1115–1123 (2005)

Wegert, M., Majer, N., Lüdge, K., Dommers-Völkel, S., Gomis-Bresco, J., Knorr, A., Woggon, U., Schöll, E.: Nonlinear gain dynamics of quantum dot optical amplifiers. Semicond. Sci. Technol. **26**(1), 014008 (2011)

Xiao, J.L., Huang, Y.Z.: Numerical analysis of gain saturation, noise figure, and carrier distribution for quantum-dot semiconductor-optical amplifiers. IEEE J. Quantum Electron. **44**(5), 448–455 (2008)

Zajnulina, M., Lingnau, B., Lüdge, K.: Four-wave mixing in quantum-dot semiconductor optical amplifiers: a detailed analysis of the nonlinear effects. IEEE J. Sel. Top. Quantum Electron. **23**(6), 1–12 (2017)

Zhang, Z., Jiang, Q., Hogg, R.: Simultaneous three-state lasing in quantum dot laser at room temperature. Electron. Lett. **46**(16), 1155–1157 (2010)